

Correlation between S100A7 and immune characteristics, methylation, tumor stemness and tumor heterogeneity in pan-cancer and its role in chemotherapy resistance in breast cancer

Yilun Li¹, Xiaolu Yang¹, Tingting Jin², Qiuli Li², Xiaolong Li³, Li Ma¹

¹Department of Breast Disease Center, The Fourth Hospital of Hebei Medical University, Shijiazhuang, China

²Department of Pathology, Hebei Medical University, Shijiazhuang, China

³Department of Breast Disease Center, The Fourth Hospital of Shijiazhuang, Shijiazhuang, China

Correspondence to: Li Ma; email: 47500562@hebmu.edu.cn

Keywords: S100A7, methylation, tumor stemness, heterogeneity, chemotherapy resistance

Received: November 13, 2023

Accepted: February 20, 2024

Published: March 18, 2024

Copyright: © 2024 Li et al. This is an open access article distributed under the terms of the [Creative Commons Attribution License](https://creativecommons.org/licenses/by/4.0/) (CC BY 4.0), which permits unrestricted use, distribution, and reproduction in any medium, provided the original author and source are credited.

ABSTRACT

Objective: To explore the relationships between S100A7 and the immune characteristics, tumor heterogeneity, and tumor stemness pan-cancer as well as the effect of S100A7 on chemotherapy sensitivity in breast cancer.

Methods: TCGA-BRCA and TCGA-PANCANCER RNA-seq data and clinical follow-up survival data were collected from the University of California Santa Cruz database. Survival analyses were performed to explore the relationship between S100A7 expression and pan-cancer prognosis. Gene Ontology (GO), Kyoto Encyclopedia of Genes and Genomes (KEGG) enrichment analyses, and Gene Set Enrichment Analysis (GSEA) were used to identify the potential pathways related to the differentially expressed genes in breast cancer. Spearman's and Wilcoxon's tests were used to investigate the relationships between S100A7 expression and immune characteristics, methylation, tumor heterogeneity, and tumor stemness. The potential functions of S100A7 and its influence on chemotherapy sensitivity in breast cancer were elucidated using reverse transcription-quantitative PCR, Cell Counting Kit-8 (CCK-8) assay, Transwell assay, and wound healing assay.

Results: S100A7 was highly expressed in most types of tumors and was associated with poor prognosis. S100A7 was closely associated with immunomodulators, immune checkpoint and immune cell infiltration. Further, S100A7 was related to tumor mutational burden, tumor heterogeneity, methylation and tumor stemness in breast cancer. High S100A7 expression was associated with the invasiveness, migration, proliferation and chemotherapy resistance of breast cancer cells *in vitro* experiments.

Conclusion: High S100A7 expression was related with poor prognosis and chemotherapy resistance in breast cancer, making it a potential immune and chemotherapy resistance biomarker.

INTRODUCTION

Breast cancer is the most common cancer in women. The incidence and mortality rates of breast cancer are extremely high; about 287,850 American and 429,150 Chinese women were diagnosed last year, with mortality often as high as 15% [1]. Today, breast cancer treatment includes radiotherapy, chemotherapy,

endocrine therapy, and anti-human epidermal growth factor receptor-2 therapy. Although these treatments are widely available, much effort is still needed to reduce the incidence and mortality of breast cancer.

Cancer biomarkers are important in cancer diagnosis, prognosis, epidemiological research, and therapeutic

intervention. Biomarkers can be used to enhance the accuracy of targeted therapies [2]. Discovering new tumor biomarkers that can predict and improve the prognosis of breast cancer is essential.

The S100 protein family, comprising 25 known members in humans, is one of the largest groups of calcium-binding proteins, all of which structurally belong to the EF-hand family [3]. These proteins are expressed in a cell- and tissue-specific manner and exert a wide range of intracellular and extracellular functions, including regulation of the cell cycle, cell proliferation, migration, invasion, phosphorylation, cytoskeletal components, and transcription factors [4]. They can produce these effects by interacting with different receptors, the most studied among which is the receptor for advanced glycation end products [5, 6]. Some members of this family, such as S100A4, S100A8/A9, S100P, and S100B, mediate the interaction between tumor and stromal cells, and thus, have been implicated in tumor progression, angiogenesis, and metastasis [7]. Naturally then, some S100 proteins have been proposed as novel targets for cancer therapy.

S100A7, also known as psoriasin, was one of the most abundant proteins detected in psoriatic keratinocytes [8]. S100A7 was found to be closely related to various tumors, such as oral squamous cell carcinoma, breast cancer, prostate cancer, osteosarcoma, head and neck cancer, lung cancer, and ovarian cancer [5, 9, 10]. Functional studies showed that S100A7 promoted cell proliferation, migration, invasion, angiogenesis, and metastasis [9, 10]. S100A7 can be induced by inflammatory cytokines and can also induce apoptosis and the expression of inflammatory cytokines/chemokines, suggesting that it may act as a stromal factor [11]. In addition, it may promote the growth of breast cancer by upregulating the pro-inflammatory pathway to recruit tumor-associated macrophages for metastasis [10]. However, the role of S100A7 in regulating tumor immunity in other types of cancer is still unknown.

As a dynamic system, cancer is characterized by the dysregulation of proliferation, survival, and growth of transformed cells. Accumulating evidence suggests that transformed cells within tumors are heterogeneous, and they undergo stochastic genetic and epigenetic alterations to enhance the fitness of subsets [12, 13]. Tumor stemness is closely related to tumor heterogeneity. Cancer cells acquire genetic mutations during tumor evolution or transformation, leading to the accumulation of subclonal populations with different phenotypes and heterogeneous features [14]. Besides, individual clones may serve different functions within populations, which points toward

nongenetic determinants that play a crucial role in shaping the differences in cellular subclones or lead to different survival outcomes in response to treatment regimens [15]. The relationship among S100A7, tumor heterogeneity, and tumor stemness is still obscure. This relationship must be studied to better understand the factors that drive intratumoral heterogeneity and tumor progression.

Methylation plays an important role in cancer progression. The expression of oncogenes increases when they are demethylated in their promoter region, leading to drug resistance. Thymosin β 4, which was overexpressed after DNA demethylation and histone H3 modification in the promoter region of its gene, conferred cancer stem cell-like ability upon hepatoma cells, making them resistant to sorafenib [16]. RNA methylation accounts for more than 60% of all RNA modifications. The 5' cap and 3' polyA modifications of eukaryotic mRNAs play a crucial role in transcriptional regulation, whereas the internal modifications help maintain mRNA stability. N⁶-methyladenosine (m⁶A), 5-methylcytosine (m⁵C), and N¹-methyladenosine (m¹A) are the most common internal mRNA modifications in eukaryotes, which impact mRNA splicing, transport, and translation [17]. The relationship between S100A7 and methylation is still unknown, and studying it can help define the factors that drive tumor progression.

In this study, we first explored the pan-cancer differences in S100A7 expression. Next, we identified the relationship between S100A7 expression and pan-cancer prognosis. Subsequently, we analyzed the immune characteristics, methylation, tumor stemness, and heterogeneity in pan-cancer. Finally, *in vitro* experiments were performed to validate the potential function of S100A7 in breast cancer.

METHODS

Data collection

The Cancer Genome Atlas-breast cancer cohort (TCGA-BRCA) and pan-cancer RNA-seq data were collected from the University of California Santa Cruz database (<https://xenabrowser.net/>) and converted into the transcripts per million formats. Data on the clinical follow-up survival and clinicopathological characteristics were simultaneously downloaded. To reduce bias in the statistical analysis, BRCA and pan-cancer patients with missing overall survival data or a follow-up time <30 days and male BRCA patients were excluded. The tumor mutational burden (TMB) and mutant-allele tumor heterogeneity (MATH) scores were calculated.

Differential and survival analysis

To ensure the accuracy of the following analysis, we deleted duplicated and missing RNA-seq data, and converted the remaining data into the $\log_2(\text{transcripts per million} + 1)$ format. Differential *S100A7* expression between normal and tumor tissues was identified using Wilcoxon rank-sum test, and samples were classified into two groups based on the median *S100A7* expression.

The relationship between *S100A7* expression and pan-cancer prognosis was examined using log-rank analysis. Cox analysis was performed to ensure the precision of the results, which were depicted as heatmaps and forest plots. The “Survminer” and “Survival” packages were used to perform survival analysis and plot survival curves.

Enrichment analysis

To clarify the impact of *S100A7* expression on some potential pan-cancer pathways, Gene Set Enrichment Analysis (GSEA) was performed, and the results were displayed in the form of a heatmap.

We also explored the impact of *S100A7* expression specifically in breast cancer. Gene Ontology analysis was performed to identify the molecular functions, biological processes, and cellular components that were enriched in breast cancer. Kyoto Encyclopedia of Genes and Genomes enrichment analysis and GSEA could predict the pathways related to *S100A7* alteration-associated genes in breast cancer. The protein–protein interaction network was also elucidated to understand the interactions between proteins associated with *S100A7* alterations in breast cancer. Finally, we compared the scores of the common pathways between the *S100A7*-high-expression and the *S100A7*-low-expression groups.

Immunomodulatory, immune cell infiltration, immune checkpoint, and immune activity score analysis

We assessed the correlations between *S100A7* expression and immunomodulators, immune checkpoints, and immune cell infiltration. Lists of genes encoding immune checkpoints and immunomodulators were downloaded from TISIDB (<http://cis.hku.hk/TISIDB/download.php>). We also compared immunomodulatory scores between the *S100A7*-high-expression and the *S100A7*-low-expression groups to further define the relationship between *S100A7* expression and immunomodulators.

The immune cell infiltration score was calculated by multiple methods (TIMER, EPIC, MCP-COUNTER, CIBERSORT, CIBERSORT-ABS, QUANTISEQ, XCELL, TIDE) and downloaded from TIMER2.0 (<http://timer.cistrome.org/>). Heatmaps were used to

illustrate the relationship between immune cell infiltration and *S100A7* expression pan-cancer. The ESTIMATE method was also used to perform the same analysis pan-cancer as well as in breast cancer.

Tracking Tumor Immunophenotype (<http://biocc.hrbmu.edu.cn/TIP/>) was used to calculate the immune activity score. We compared the immune activity scores between the *S100A7*-high and -low expression groups to establish the relationship between *S100A7* expression and immune activity.

Finally, we performed a pan-cancer correlation analysis between *S100A7* expression and immune checkpoints. We also compared immune checkpoint scores between the *S100A7*-high and -low expression groups.

Association with m⁶A, m⁵C, m¹A, and DNA methylation

A correlation analysis was performed between *S100A7* expression and m⁶A, m⁵C, m¹A, and DNA methylation. DNA methylation data were downloaded from the Gene Set Cancer Analysis database (<http://bioinfo.life.hust.edu.cn/GSCA/>). The m⁶A, m⁵C, and m¹A gene sets were downloaded from the literature (<https://doi.org/10.3389/fimmu.2022.918140>).

Gene mutation, tumor stemness, and tumor heterogeneity analysis

TMB and MATH were used to predict the efficacy of tumor immunotherapy and tumor heterogeneity. The “maftools” package was used for calculating TMB and MATH scores in breast cancer [18]. We also downloaded microsatellite instability, neoantigen, and purity scores from the literature to examine the relationship between *S100A7* expression and tumor heterogeneity [19, 20].

Six tumor stemness scores—RNA expression-based stemness score (RNAss), epigenetically regulated RNA expression-based stemness score (EREG.EXPss), DNA methylation-based stemness score (DNAss), epigenetically regulated DNA methylation-based stemness score (EREG-METHss), differentially methylated probes-based stemness score (DMPss), and enhancer elements/DNA methylation-based stemness score (ENHss)—were downloaded from the literature [21]. The relationship between *S100A7* expression and tumor stemness was analyzed using Spearman’s method.

We downloaded the level 4 single nucleotide variation dataset for TCGA samples processed using Mutect2 [22] and the level 4 copy number variation dataset for all TCGA samples processed using GISTIC [23]. Samples with synonymous mutations were filtered, and

$\log_2(\times + 0.001)$ transformation was applied to each expression value. Finally, tumors with less than three samples in a single cancer were excluded. The data so processed were used to study the relationship among single nucleotide variation, copy number variation, and *S100A7* expression.

We also evaluated the relationship between gene mutation and *S100A7* expression. The “maftools” package was used to analyze mutation-related data and to visualize this relationship in breast cancer. All these results were visualized using the “ggplot2” and “ggpubr” packages.

Experimental material

Cell Counting Kit-8 (CCK8) was purchased from MedChemExpress (Monmouth Junction, NJ, USA). CellTiter 96[®] Aqueous One Solution Reagent Kit for measuring the cell viability was obtained from Promega Co. (Madison, WI, USA). Lipofectamine 3000 was bought from Invitrogen Co. (Carlsbad, CA, USA). The *S100A7* expression plasmid with the green fluorescent protein tag (pGensil-1-*S100A7*) was designed by Sangon Biotech Co. (Shanghai, China).

Cell culture

MCF7 and MDA-MB-231 cells were purchased from the Cell Resource Center, Institute of Basic Medicine, Chinese Academy of Medical Sciences and Peking Union Medical College. They were cultured in DMEM (containing 4.5 g of glucose; Gibco, Waltham, MA, USA) containing 10% fetal bovine serum (FBS; Gibco) and 1% penicillin/streptomycin (Gibco) at 37°C in a humidified incubator having 5% CO₂.

Cell transfection

MCF7 and MDA-MB-231 cells were seeded in 6-well plates and transfected at 90% confluence with the indicated plasmid using Lipofectamine 3000, according to the manufacturer’s instructions. Briefly, 2.5 µg of the plasmid was mixed with 5 µL of P3000 in 125 µL of serum-free DMEM. Separately, 5 µL of Lipofectamine 3000 was mixed in 125 µL of serum-free DMEM. These two mixtures were complexed for 15 min at room temperature before they were added to the cells. The transfection efficiency was evaluated 48 h later under an inverted fluorescence microscope.

Reverse transcription-quantitative PCR

Total RNA was extracted from MCF7 and MDA-MB-231 cells using TRIzol reagent (Takara, Dalian, China), and cDNA was synthesized according to the

instructions of the Reverse Transcription Kit (Takara). Based on the Ct value, the expression of the target gene was calculated by the $2^{-\Delta\Delta Ct}$ method.

CCK8 assay

MCF7 or MDA-MB-231 cells in their growth phase were seeded in 96-well cell culture plates at a density of 5000 cells/100 µL of medium and cultured for 24 h at 37°C. The drug concentrations tested on MDA-MB-231 cells were 0, 1, 2, 4, 5, and 8 mg/L, whereas those tested on MCF7 cells were 0, 0.1, 0.2, 0.25, 0.4, and 0.5 mg/L. After 48 h of culture, the cells were incubated with 10 µL of CCK8 reagent for 2 h, following which the absorbance was measured at 450 nm. The inhibition rate was calculated according to the following formula: inhibition rate = (1-experimental group/control group). Finally, the half-maximal inhibitory concentration (IC₅₀) was calculated.

We also used the CCK8 assay to evaluate cell proliferation. MCF7 and MDA-MB-231 cells were seeded in 96-well cell culture plates as described above. The absorbance was measured at 450 nm at 0 h, 24 h, 48 h, and 72 h to evaluate the susceptibility of *S100A7* expression to breast cancer cell proliferation and chemosensitivity. We calculated the percentage of cell viability. Cell viability was calculated as follows:

$$\text{Cell viability (\%)} = \frac{OD450(\text{treatment group}) - OD450(\text{blank})}{OD450(\text{control group}) - OD450(\text{blank})} \times 100\%$$

Treatment group: Containing cells and different concentrations of drugs (include 0) in knockdown or control groups.

Control group: Only containing cells in knockdown or control groups.

Blank: Both cells and drugs were not contained in knockdown or control groups.

Transwell assay

To test the migration ability of breast cancer cells, suspensions of MCF7 and MDA-MB-231 cells were prepared in DMEM without FBS at a density of 2×10^4 cells/mL. The upper chamber of the Transwell was filled with 100 µL of this suspension, while the lower chamber was filled with 500 µL of DMEM containing FBS. The excess cells were retrieved with a sterile cotton swab, fixed in 4% formaldehyde, and stained with 0.1% crystal violet to count the number of migrating cells.

To investigate the invasiveness of MCF7 and MDA-MB-231 cells, the stroma was diluted in DMEM without FBS at a ratio of 1:7 (Beyotime, Guangzhou, China). An aliquot of 50 µL was aspirated into the upper chamber

and allowed to rest for 3–4 h. The rest of the procedure was the same as that described for the migration assay.

Wound healing assay

For this experiment, 1×10^6 cells per well were seeded in 6-well plates. After cell transfection and overnight incubation, the cells were scratched using a 10- μ L pipette tip and photographed using a powered microscope with a 4 \times magnification at 0 h and 24 h.

Statistical analysis

T-test was used to compare two groups of measurement data. The Wilcoxon rank-sum and Kruskal tests were employed to identify the differences in three clusters. Univariate Cox regression was used to assess the differences between counting data. Log-rank test was used to evaluate the prognosis of cancer. $P < 0.05$ was considered statistically significant.

Availability of data and materials

The data can be downloaded from TCGA (<https://portal.gdc.cancer.gov/>). The codes used during the current study are available from the corresponding author on reasonable request.

RESULTS

S100A7 was highly expressed and associated with poor prognosis in pan-cancer

We found that *S100A7* was expressed at a significantly higher level pan-cancer (in glioblastoma multiforme, glioma, brain lower grade glioma, uterine corpus endometrial carcinoma, breast invasive carcinoma, esophageal carcinoma, stomach and esophageal carcinoma, colon adenocarcinoma, prostate adenocarcinoma, stomach adenocarcinoma, lung squamous cell carcinoma, thyroid carcinoma, rectum adenocarcinoma, ovarian serous cystadenocarcinoma, testicular germ cell tumors, all, kidney chromophobe; Figure 1A). *S100A7* was highly expressed in breast cancer as well (Figure 1B–1D).

We also explored the relationship between *S100A7* expression and pan-cancer prognosis. Log-rank test and univariate Cox regression were used to conduct survival analysis. We found that *S100A7* was related to the prognosis of multiple types of cancer (Figure 2A). *S100A7* expression was closely related to the overall survival of patients with skin cutaneous melanoma (Figure 2B), kidney renal clear cell carcinoma (Figure 2C), liver hepatocellular carcinoma (Figure 2D), and the disease-specific survival of patients with kidney

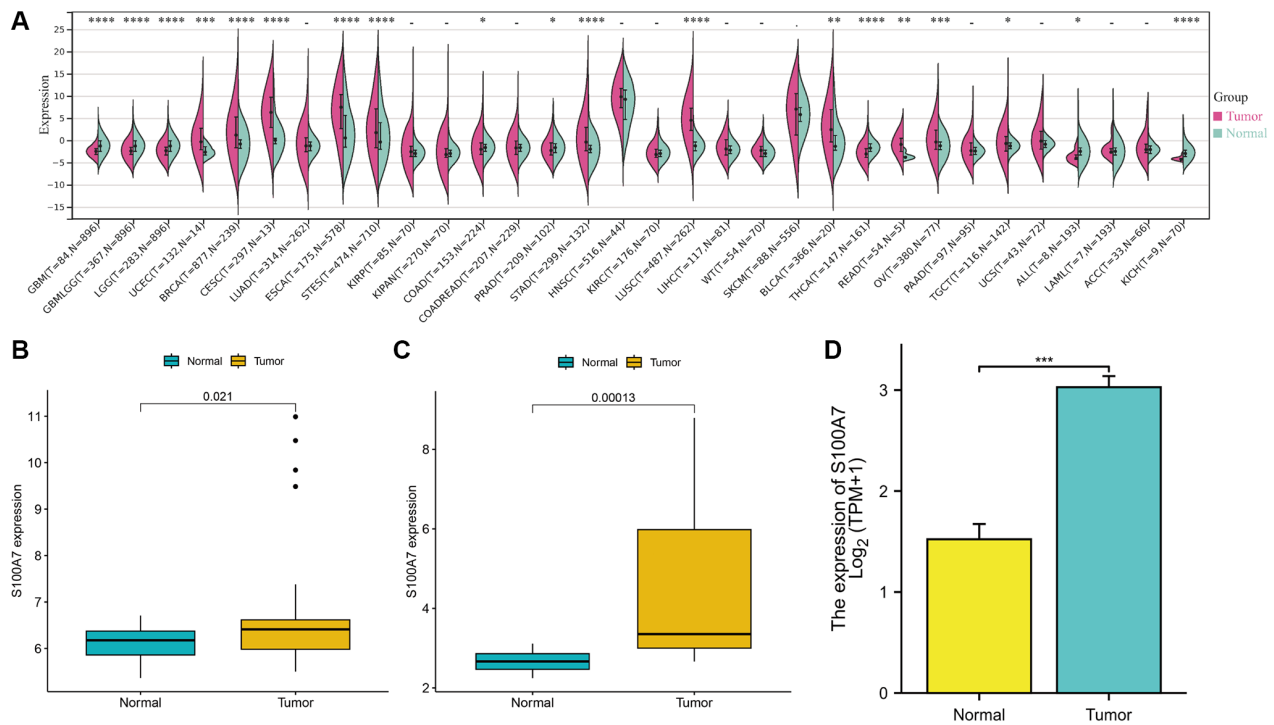


Figure 1. The pan-cancer expression of *S100A7*. (A) *S100A7* expression from TCGA + GTEx microarray data. (B) *S100A7* expression from GSE15852 data. (C) *S100A7* expression in breast cancer and normal breast tissues from GSE10797 data. (D) *S100A7* expression in breast cancer and normal breast tissues from TCGA-BRCA data. Abbreviations: TCGA: The Cancer Genome Atlas; GTEx: Genotype-Tissue Expression.

renal clear cell carcinoma (Figure 2E) and skin cutaneous melanoma (Figure 2F). What's more, *S100A7* expression was closely related to the overall survival of patients with bladder urothelial carcinoma (Figure 2G).

Enrichment analysis revealed that *S100A7* was related to multiple cancer development pathways

We performed enrichment analyses to investigate the potential pathways affected by *S100A7* pan-cancer and

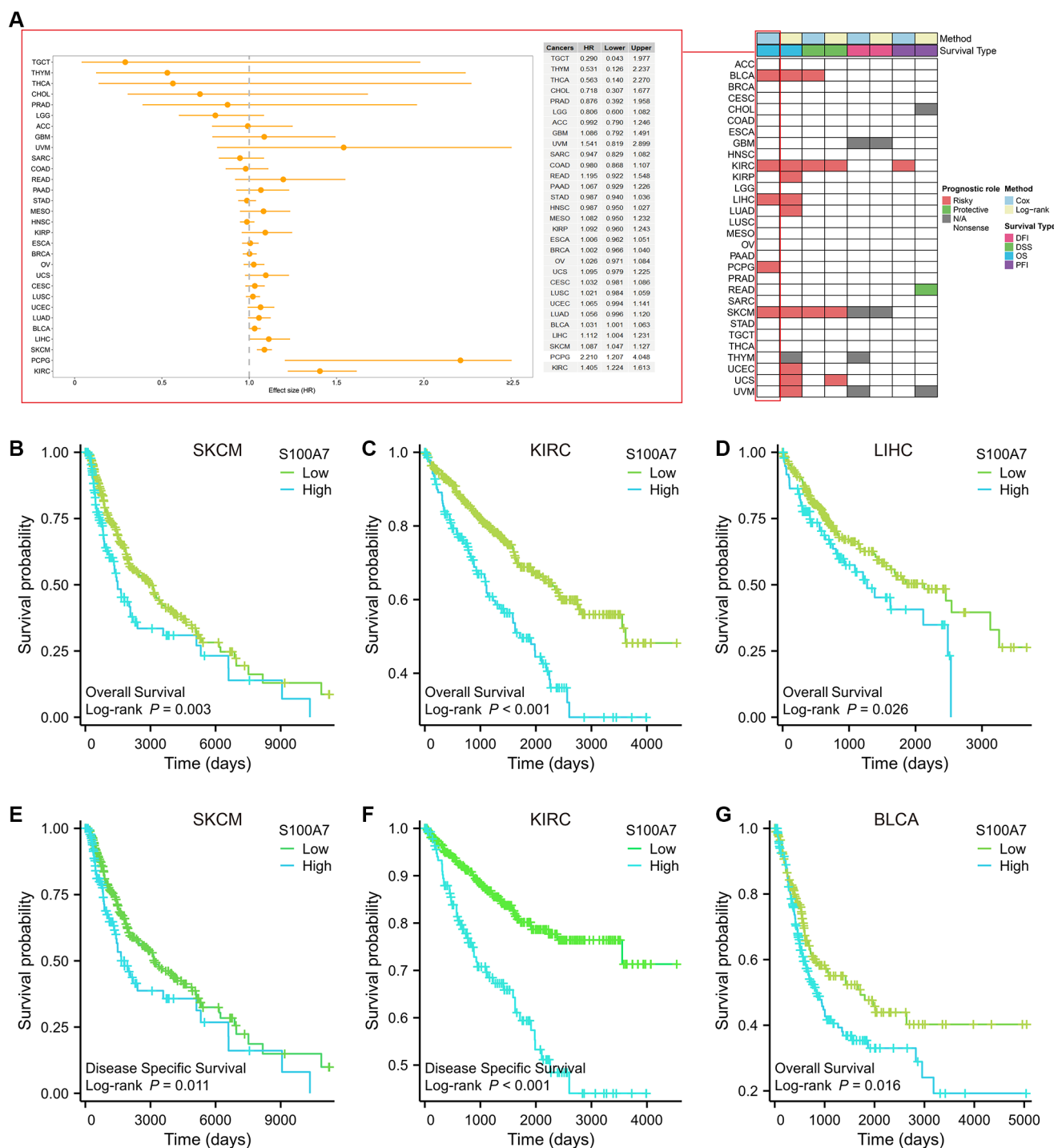


Figure 2. Relationship between *S100A7* expression and the prognostic value of *S100A7* pan-cancer. (A) The pan-cancer prognostic value of *S100A7* (univariate Cox and log-rank analysis). Prognostic value of *S100A7* expression in terms of OS in (B) SKCM, (C) KIRC, (D) LIHC, and DSS in (E) SKCM and (F) KIRC. It also reflected the prognostic value of *S100A7* expression in terms of OS in (G) BLCA. Abbreviations: OS: overall survival; DSS: disease-specific survival; SKCM: skin cutaneous melanoma; KIRC: kidney renal clear cell carcinoma; LIHC: liver hepatocellular carcinoma; BLCA: bladder urothelial carcinoma.

closely related to RNA processing, the nucleolus, signaling receptor activity, and the nicotine addiction pathway (Figure 4C, 4D). The protein–protein interaction network of all differentially expressed genes was charted to understand the interaction among them (Figure 4E).

***S100A7* affects immunomodulators, immune cell infiltration, immune activity score, and immune checkpoints**

We examined the relationship between *S100A7* and tumor immunity. Spearman’s correlation analysis showed that *S100A7* was closely related to immunomodulators pan-cancer (Figure 5A). In breast cancer, *S100A7* was associated with immunomodulators (Figure 5B),

the major histocompatibility complex (Figure 5C), chemokines (Figure 5D), and receptors (Figure 5E).

Multiple methods were used to assess the correlation between immune cell infiltration and *S100A7* expression pan-cancer. *S100A7* was associated with B cells, CD4⁺ T cells, CD8⁺ T cells, cancer-associated fibroblasts, macrophages, neutrophils, and mast cells (Figure 6). The immune, stromal, and ESTIMATE scores were also related to *S100A7* expression pan-cancer (Figure 7A) as well as in breast cancer (Figure 7B–7D).

Further, the immune activity score was higher in the *S100A7*-high than in the *S100A7*-low expression group (Figure 7E).

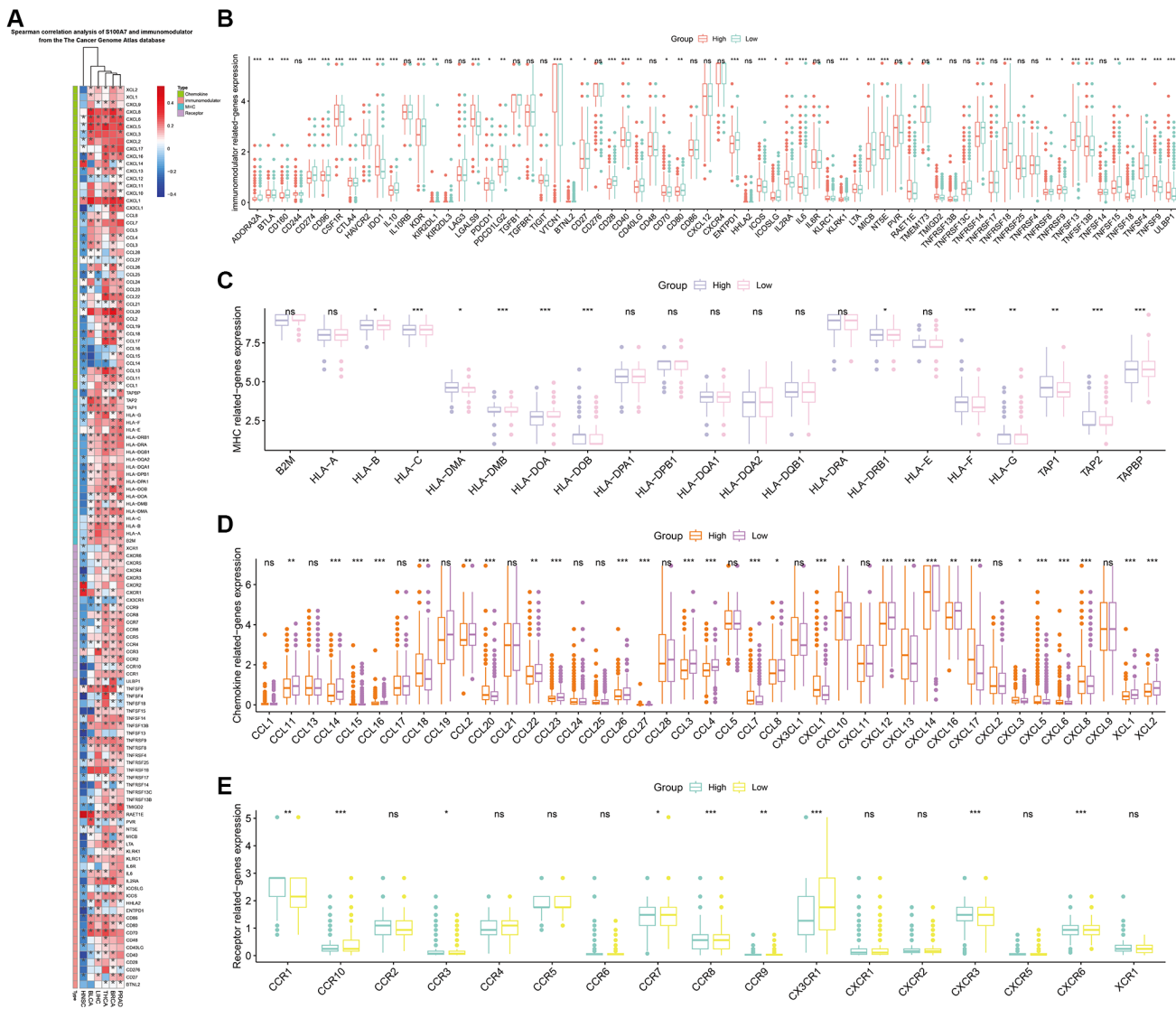


Figure 5. Correlation between *S100A7* expression and immunomodulators in pan-cancer. (A) Correlation between *S100A7* expression and immunomodulators in pan-cancer. The expression of genes related to immunomodulators (B), MHC (C), chemokines (D), and receptors (E) in the two groups based on the median *S100A7* expression in breast cancer. “ns” represents not significant. **P* < 0.05; ***P* < 0.01; ****P* < 0.001. Abbreviation: MHC: major histocompatibility complex.

Finally, correlation analysis showed that *S100A7* was related to immune checkpoints pan-cancer (Figure 7F). A comparison of the expression of immune checkpoints

between the *S100A7*-high and -low expression groups further verified the close association between *S100A7* expression and immune checkpoints (Figure 7G, 7H).

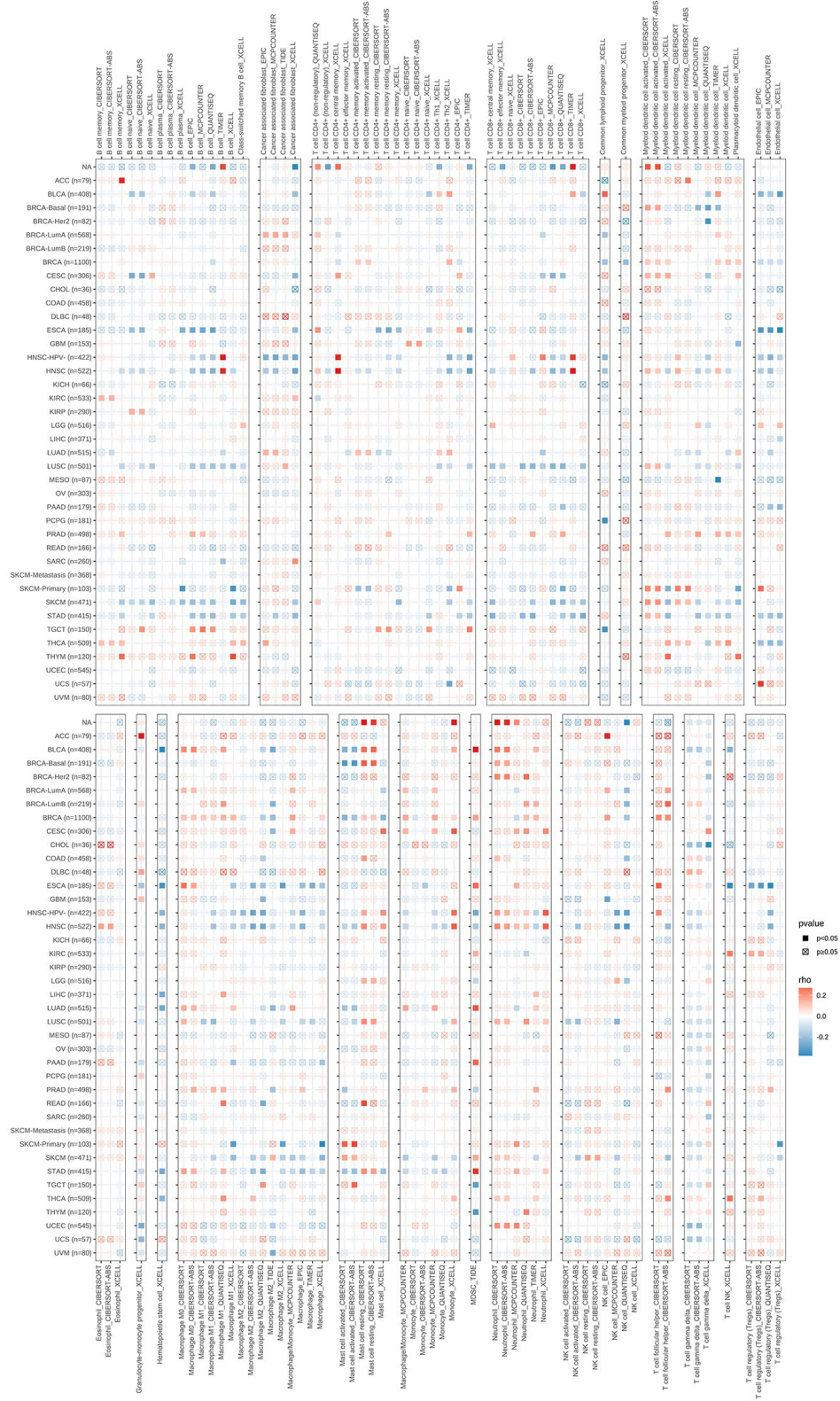


Figure 6. Correlation between *S100A7* expression and immune cell infiltration pan-cancer. “x” represents $P > 0.05$, which was not statistically significant.

***S100A7* is associated with methylation, gene mutation, tumor heterogeneity, and stemness**

We also studied the relationship between methylation and *S100A7* expression in cancer. *S100A7* expression was closely correlated with the m⁶A, m⁵C, and m¹A modifications (Figure 8A). It was also associated with the DNA methylation sites cg00325910, cg02892624, and cg17421062 pan-cancer (Figure 8B). Moreover, the expression of m⁶A-, m⁵C-, and m¹A-related genes differed between the *S100A7*-high and -low expression groups (Figure 8C).

Next, we analyzed the differences in the gene mutation landscape of *S100A7* between the *S100A7*-high and

-low expression groups (Figure 9A). Copy number variation was similar between the two groups pancreatic cancer (Figure 9B), but single nucleotide variation was associated with *S100A7* expression (Figure 9C). In the *S100A7*-high expression group, the genes most susceptible to mutation were *TP53*, *PIL3CA*, *TTN*, *GATA3*, and *CDH1* (Figure 9D).

Finally, we explored the relationship between *S100A7* expression and tumor stemness and heterogeneity. *S100A7* expression was associated with tumor heterogeneity (TMB, MATH, microsatellite instability, neoantigen, purity, ploidy, homologous recombination deficiency (HRD), and loss of heterozygosity (LOH) scores; Figure 10A). In breast cancer, the tumor

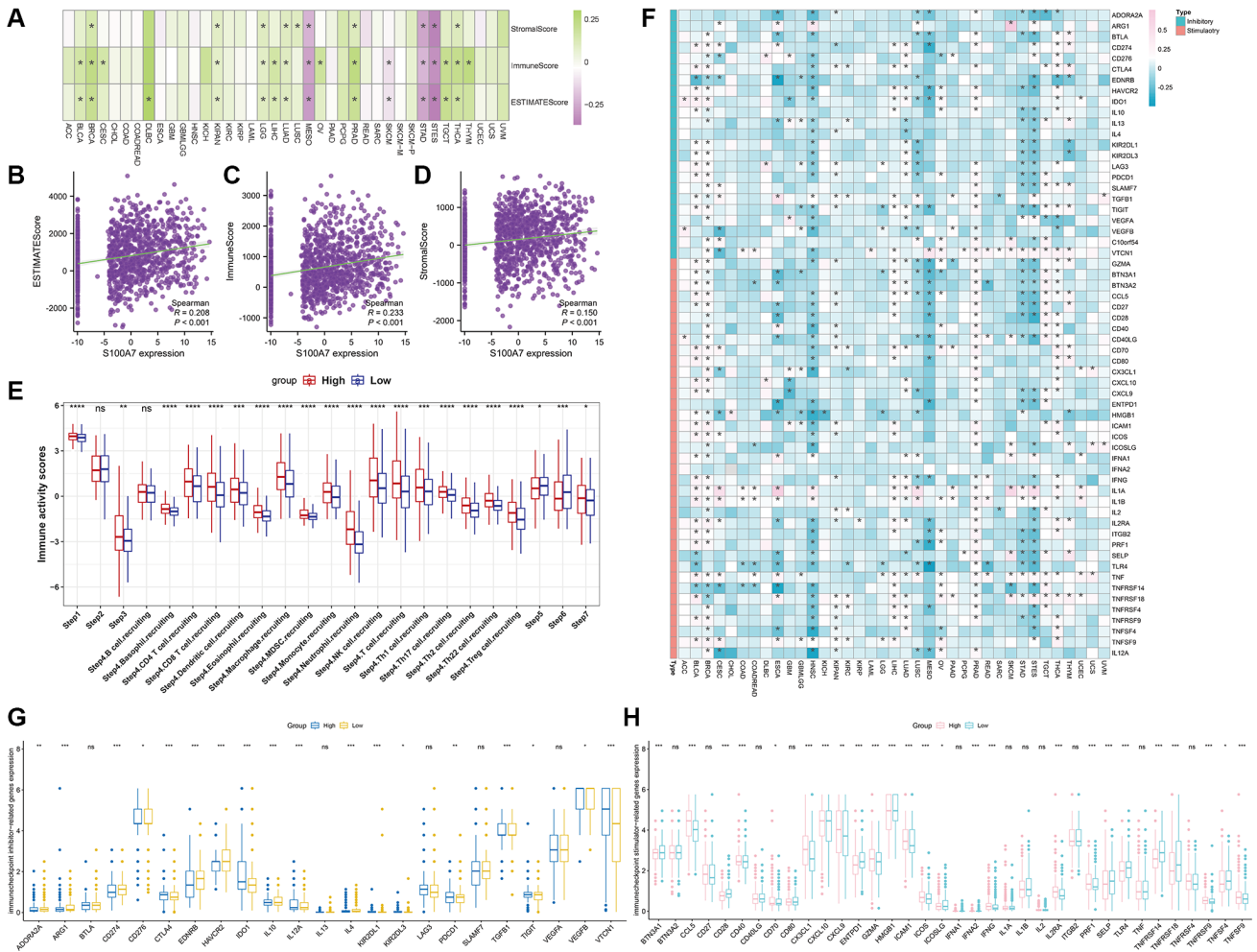


Figure 7. Correlation between *S100A7* expression and immune infiltration as well as immune checkpoints pan-cancer, and the relationship between *S100A7* expression and immune activity scores in breast cancer. (A) Correlation between *S100A7* expression and immune infiltration pan-cancer. Correlation between *S100A7* expression and the ESTIMATE score (B), immune score (C), and stromal score (D) in breast cancer. (E) Relationship between *S100A7* expression and immune activity score in breast cancer. STEP1: Release of cancer cell antigens; STEP2: Cancer antigen presentation; STEP3: Priming and activation; STEP4: Trafficking of cells to tumors; STEP5: Infiltration of immune cells into tumors; STEP6: Recognition of cancer cells by T cells; STEP7: Killing of cancer cells. (F) Correlation between *S100A7* expression and immune checkpoints pan-cancer. The expression of genes related to inhibitors (G) and stimulators (H) of immune checkpoints in the two groups based on the median *S100A7* expression in breast cancer. “ns” represents not significant. **P* < 0.05; *P* < 0.01; ****P* < 0.001.**

heterogeneity indicators that most correlated with *S100A7* expression were HRD, TMB, and LOH (Figure 10A). The tumor stemness indicators RNAss, ENHss, DMPss, DNAss, EREG-METHss, and EREG-EXPss were also associated with *S100A7* expression (Figure 10B). In breast cancer, DMPss and EREG-EXPss were associated with *S100A7* expression (Figure 10C).

S100A7 promotes breast cancer cell proliferation, invasion, migration, and chemoresistance *in vitro*

We performed *in vitro* experiments to verify the functions of *S100A7* in cancer. The CCK8 proliferation assay showed that *S100A7* knockdown inhibited the proliferation of MCF7 and MDA-MB-231 cells

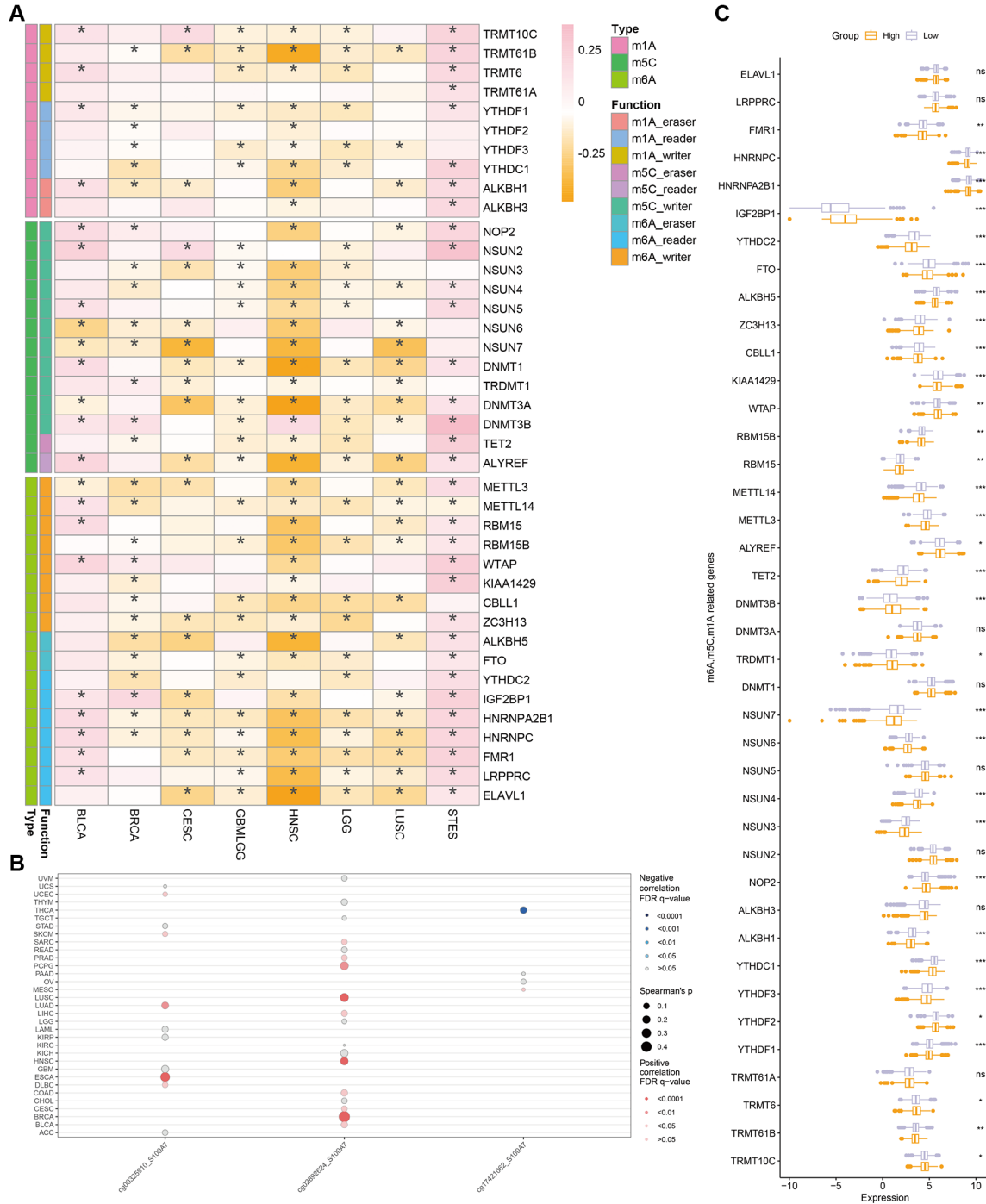


Figure 8. Correlation between methylation and *S100A7* expression pan-cancer. (A) Correlation between *S100A7* expression and m⁶A, m⁵C, and m¹A pan-cancer. (B) Correlation between DNA methylation and *S100A7* expression pan-cancer. (C) The expression of genes related to m⁶A, m⁵C, and m¹A in the two groups based on the median *S100A7* expression in breast cancer. "ns" represents not significant. **P* < 0.05; ***P* < 0.01; ****P* < 0.001. Abbreviations: m6A: N⁶-methyladenosine; m1A: N¹-methyladenosine; m5C: 5-methylcytosine.

(Figure 11A), which was accompanied by a downregulation of the proliferation biomarkers Ki67 and proliferating cell nuclear antigen (Figure 11B).

The Transwell assay demonstrated that *S100A7* was associated with the invasion and migration of breast cancer cells (Figure 11C). The migration biomarkers matrix metalloproteinases-2 and -9 were also down-regulated after *S100A7* was knocked down (Figure 11D). The wound healing assay showed that *S100A7* knockdown inhibited the migration of MCF7 and MDA-MB-231 cells (Figure 11E).

We also used Taxol to explore the relationship between *S100A7* expression and sensitivity to chemotherapy.

The CCK8 assay showed that the IC₅₀ of breast cancer cells to Taxol diminished when *S100A7* was knocked down (Figure 12A). The wound healing assay further showed that *S100A7* knockdown inhibited the migration of breast cancer cells after Taxol treatment, indicating that *S100A7* contributed to chemotherapy resistance in breast cancer (Figure 12B, 12C).

DISCUSSION

In this study, we first established the level of *S100A7* expression pan-cancer and its relationship with patient prognosis. Subsequently, we explored the relationship between *S100A7* expression and immune characteristics, methylation, tumor heterogeneity, tumor

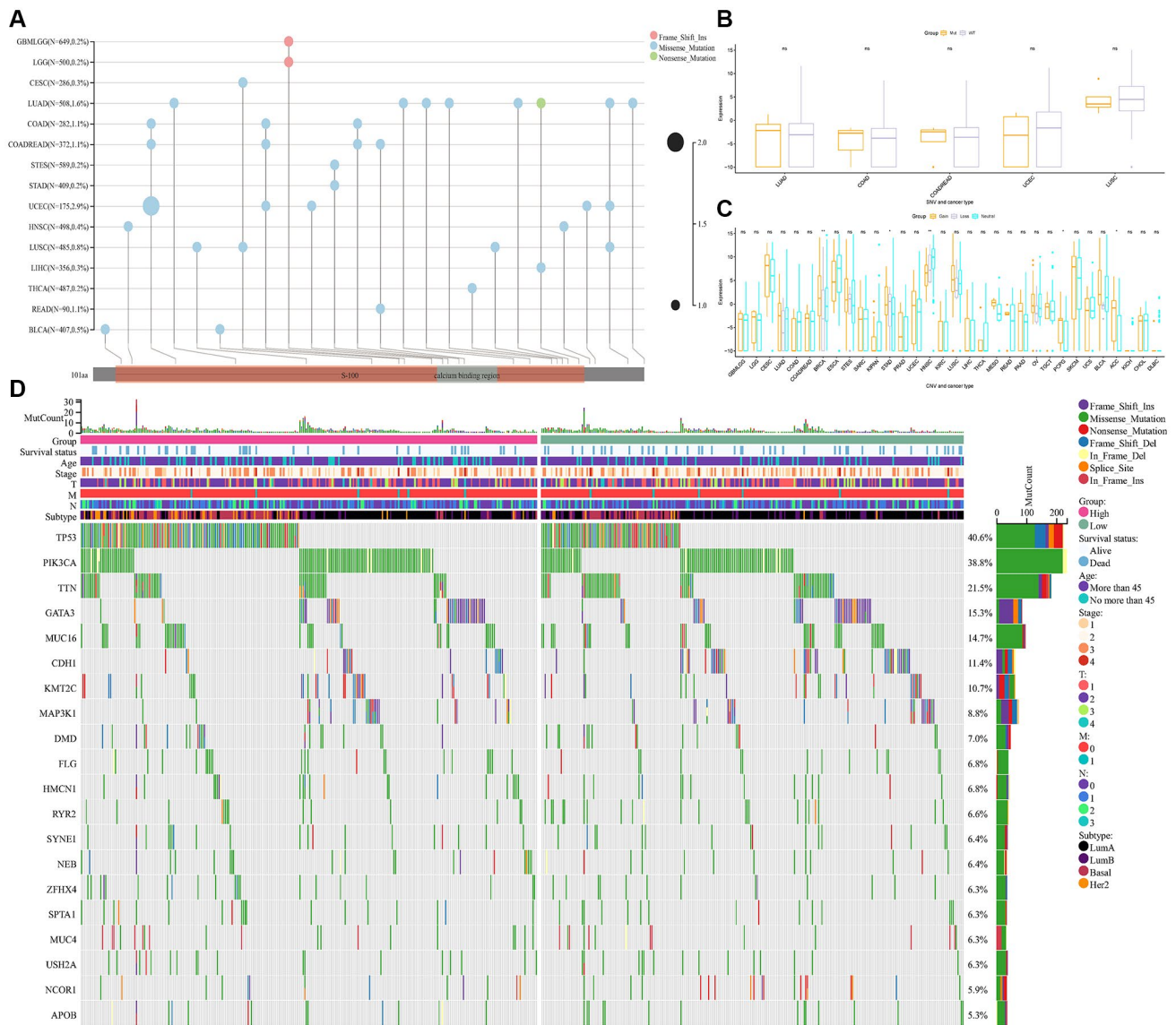


Figure 9. Relationship between gene mutation and *S100A7* expression. (A) The pan-cancer gene mutation landscape of *S100A7*. The relationship between *S100A7* expression and CNV (B) and SNV (C) pan-cancer. (D) The gene mutation landscape in the two groups based on the median *S100A7* expression in breast cancer. "ns" represents not significant. * $P < 0.05$; ** $P < 0.01$; *** $P < 0.001$. Abbreviations: CNV: copy number variation; SNV: single nucleotide variation.

maintaining specific memory lymphocytes, and eliminating autoreactive immune cells to develop self-tolerance. The homeostasis of the immune system

depends on its two major branches: the innate and the adaptive immune system, each of which is equipped with unique cells and molecules to perform its specific

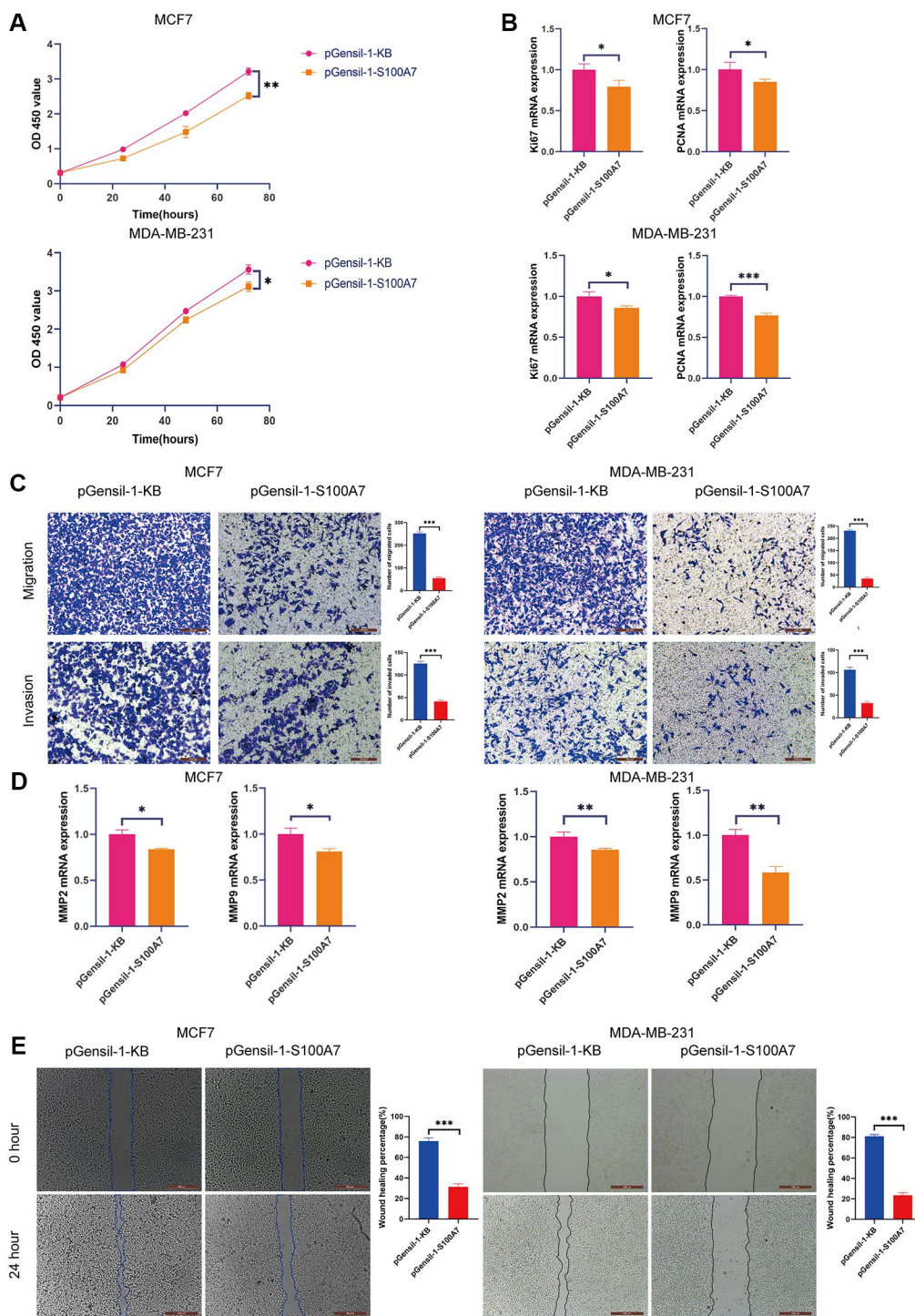


Figure 11. S100A7 promotes the proliferation, migration, and invasion of breast cancer cells *in vitro*. (A) The CCK-8 assay showed that knockdown S100A7 reduced the proliferation of MCF7 and MDA-MB-231 cells. (B) RT-qPCR showed that knockdown of S100A7 reduced the expression of the proliferation biomarkers Ki67 and PCNA. (C) The Transwell assay showed that knockdown of S100A7 attenuated the migration and invasion of MCF7 and MDA-MB-231 cells. (D) RT-qPCR showed that knockdown of S100A7 reduced the expression of the migration biomarkers MMP2 and MMP9. (E) The wound healing assay showed that knockdown of S100A7 decreased the migration of MCF7 and MDA-MB-231 cells. * $P < 0.05$; ** $P < 0.01$; *** $P < 0.001$. All experiments were repeated thrice. Abbreviations: CCK-8: Cell Counting Kit-8; RT-qPCR: reverse transcription-quantitative PCR; PCNA: proliferating cell nuclear antigen; MMP: matrix metalloproteinase.

function. These two types of immune responses are regulated by a series of cytokines, also known as immunomodulators, that are released upon receiving certain stimuli [31, 32]. In this study, we found that

S100A7 expression was negatively correlated with immunomodulators in head and neck squamous cell carcinoma, while was positively correlated in breast invasive carcinoma, liver hepatocellular carcinoma,

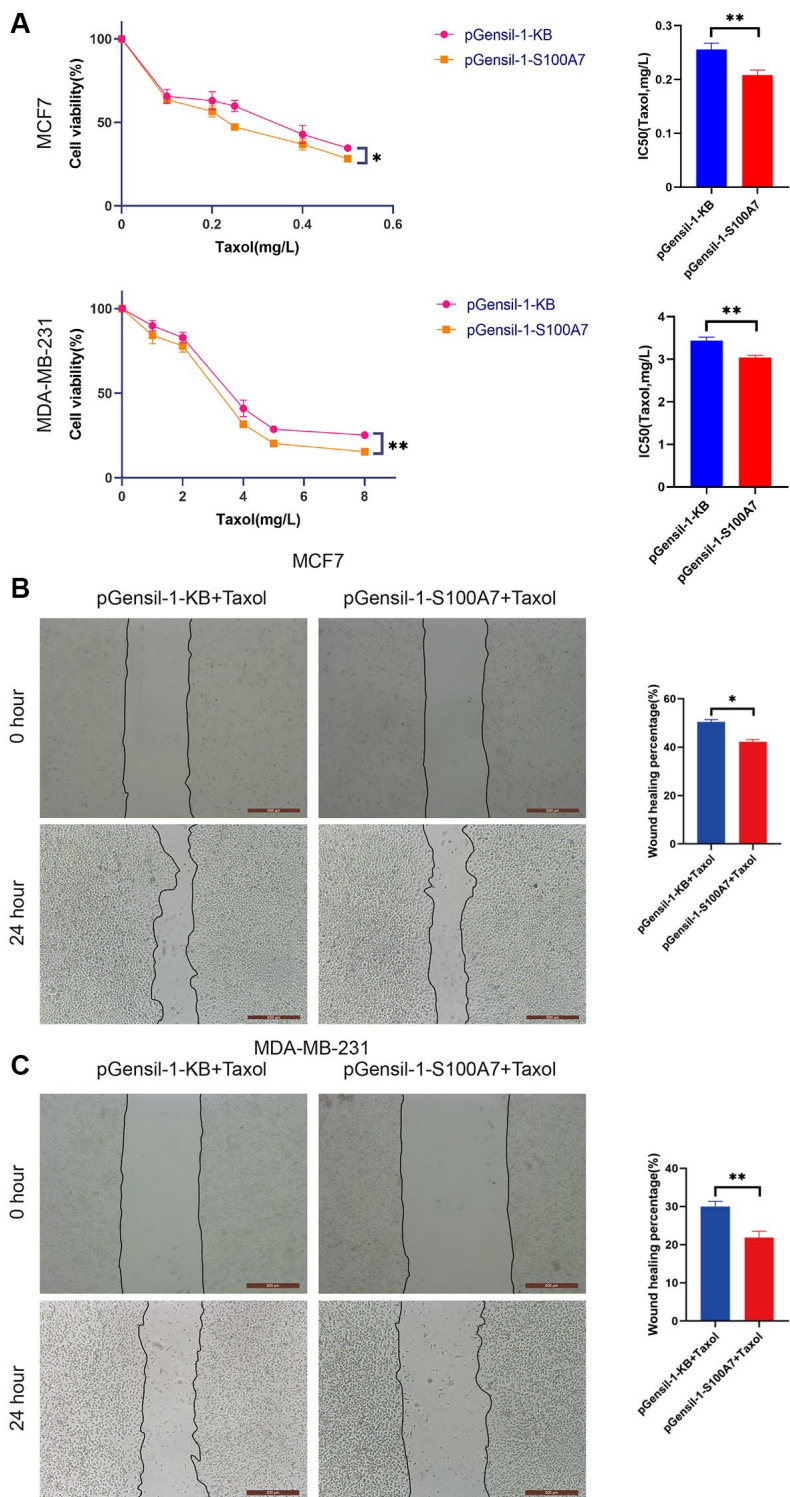


Figure 12. *S100A7* reduced the chemosensitivity of breast cancer cells *in vitro*. (A) The CCK-8 assay showed that knockdown of *S100A7* reduced the IC₅₀ of MCF7 and MDA-MB-231 cells towards Taxol. The wound healing assay showed that knockdown of *S100A7* inhibited the migration of (B) MCF7 and (C) MDA-MB-231 cells after Taxol treatment (MCF7: 0.05 mg/L, MDA-MB-231: 1 mg/L). **P* < 0.05; ***P* < 0.01; ****P* < 0.001. All experiments were repeated thrice. IC₅₀, half-maximal inhibitory concentration.

prostate adenocarcinoma and thyroid carcinoma. *S100A7* was also correlated with the expression of programmed cell death-ligand-1 in multiple types of cancer. Due to tumor heterogeneity, the effect of *S100A7* on immunomodulators, immune activity and infiltration varies across in different tumor types. What's more, the regulatory effects of *S100A7* on immunomodulators, immune activity, and infiltration could vary across different types of cancer. Previous studies had confirmed that *S100A7* expression could facilitate the infiltration of tumor-associated macrophages through multiple mechanisms in breast cancer, for example, it facilitated the infiltration of CD163-positive tumor-associated macrophages through activation of cPLA2 [33]. Furthermore, *S100A7* could facilitate the secretion of immunomodulators, including IL-6, in tumors and tumor-associated immune cells, thereby enhancing tumor infiltration [34]. Additionally, Previous evidence had shown that *S100A7* could interact with advanced glycosylation end product receptor (RAGE) and Toll-like receptor 4 (TLR4), thereby exerting paracrine effects and promoting the infiltration of macrophage in breast cancer [35]. However, accumulating evidence suggested that *S100A7* was negatively correlated with immune infiltration and immunomodulators in the lung cancer, for instance, expression of *S100A7* could inhibit PD-L1, leading to down-regulating CD68+ macrophage infiltration [36]. These results highlight the important role played by *S100A7* through its interaction with immunomodulators.

Methylation affects the development of cancer. DNA methylation refers to the transfer of active methyl groups to specific bases in a DNA chain. S-adenosylmethionine serves as the methyl donor, and the process is catalyzed by DNA methyltransferase [37]. Aberrant DNA methylation is closely related to the occurrence and development of tumors. The methylation of tumor suppressor genes and DNA repair genes leads to their silencing, which eventually results in increased gene damage. On the other hand, a reduction in the overall methylation of the genome activates proto-oncogenes and retrotransposons and reduces chromosome stability [38]. RNA methylation involves the methylation of adenine (A), guanine (G), or cytosine (C) on an RNA molecule. The most common RNA methylations are m⁶A, m¹A, and m⁵C [39]. m⁶A, which involves the addition of a methyl group to the N atom at position 6 of adenosine, is the most abundant chemical modification of RNA transcripts. The main function of the m⁶A modification is to affect the translation and stability of the RNA. The methylation happens at the N1 site of adenosine in m¹A, while it happens on the fifth C atom of cytosine in m⁵C [37–39]. RNA methylation plays an important role in regulating biological processes like tumor cell

proliferation and apoptosis. Besides, it can affect tumor progression and prognosis by affecting the function of tumor immune cells and the TME. This study showed that *S100A7* was closely related to methylation in multiple types of cancer, suggesting that it may play an important role in executing this modification.

Tumor stemness and heterogeneity are important factors affecting the development and treatment of cancer. Stemness is defined as the potential of the cells of origin to self-renew and differentiate. Cancer stem cells are cancer cells with characteristics associated with normal stem cells, in particular the ability to give rise to all tumor cell types. Cancer stem cells are thought to be responsible for tumor growth and maintenance because they are usually resistant to conventional chemotherapy and radiotherapy and are involved in tumor metastasis and recurrence [40]. A single clone may show functional variation in the population [16], reflecting tumor heterogeneity, which crucially impacts the potential function and behavior of tumor cells and ultimately affects cancer progression and its response to treatment. We demonstrated that *S100A7* was closely associated with the indicators of tumor heterogeneity (TMB, MATH, purity, HRD, and LOH) as well as those of tumor stemness (RNAss, DNAss, and EREG.EXPss) in multiple types of cancer, implying that *S100A7* could play an important role in influencing these two features of tumors.

Chemotherapy can effectively kill rapidly growing tumor cells and is widely used in cancer treatment. However, some patients still face poor prognosis, and about 90% of treatment failure cases are related to chemotherapy resistance. Several factors underlie the development of chemotherapy resistance, including methylation, the TME, tumor heterogeneity, and tumor stemness [27, 41]. Since *S100A7* was closely associated with all these factors, we hypothesized that it might be involved in the development of chemotherapy resistance in breast cancer. Through *in vitro* experiments, we found that the IC₅₀ of breast cancer cells to Taxol decreased when *S100A7* was knocked down, indicating that *S100A7* was indeed closely related to chemotherapy resistance in breast cancer.

CONCLUSION

This study elucidated the relationship between *S100A7* expression and tumor stemness, tumor heterogeneity, methylation, and chemotherapy sensitivity. These results provide a reference for exploring novel mechanisms of *S100A7* pan-cancer as well as in breast cancer, and they can help inform regimens of personalized treatment.

AUTHOR CONTRIBUTIONS

L.M. conceptualized and designed the study, revised the manuscript, and approved the final version. Y.L. and X.Y. performed experiments. Y.L. analyzed the data, interpreted the results, and wrote the manuscript. T.J., Q.L., X.Y., and X.L. collected the data.

CONFLICTS OF INTEREST

The authors declare no conflicts of interest related to this study.

ETHICAL STATEMENT

This study was approved by Ethics Committee of the Fourth Hospital of Hebei Medical University. The ethics number of this study is 2023KS003.

FUNDING

This research was supported by the Foundation of Hebei Province for the Scientific Research of Selected Returned Overseas Professionals (No. CY201608), Clinical Medical Talent Support Program of Hebei Provincial Department of Finance (No. 201746), and the Innovation Team Support Plan of the Fourth Hospital of Hebei Medical University (2023B01).

REFERENCES

1. Siegel RL, Miller KD, Wagle NS, Jemal A. Cancer statistics, 2023. *CA Cancer J Clin.* 2023; 73:17–48. <https://doi.org/10.3322/caac.21763> PMID:[36633525](https://pubmed.ncbi.nlm.nih.gov/36633525/)
2. Wang W, Liu X, Zhang C, Sheng F, Song S, Li P, Dai S, Wang B, Lu D, Zhang L, Yang X, Zhang Z, Liu S, et al. Identification of two-dimensional copper signatures in human blood for bladder cancer with machine learning. *Chem Sci.* 2022; 13:1648–56. <https://doi.org/10.1039/d1sc06156a> PMID:[35282611](https://pubmed.ncbi.nlm.nih.gov/35282611/)
3. Donato R, Cannon BR, Sorci G, Riuzzi F, Hsu K, Weber DJ, Geczy CL. Functions of S100 proteins. *Curr Mol Med.* 2013; 13:24–57. PMID:[22834835](https://pubmed.ncbi.nlm.nih.gov/22834835/)
4. Bresnick AR, Weber DJ, Zimmer DB. S100 proteins in cancer. *Nat Rev Cancer.* 2015; 15:96–109. <https://doi.org/10.1038/nrc3893> PMID:[25614008](https://pubmed.ncbi.nlm.nih.gov/25614008/)
5. Tian T, Li X, Hua Z, Ma J, Wu X, Liu Z, Chen H, Cui Z. S100A7 promotes the migration, invasion and metastasis of human cervical cancer cells through epithelial-mesenchymal transition. *Oncotarget.* 2017; 8:24964–77. <https://doi.org/10.18632/oncotarget.15329> PMID:[28212564](https://pubmed.ncbi.nlm.nih.gov/28212564/)
6. Leclerc E, Vetter SW. The role of S100 proteins and their receptor RAGE in pancreatic cancer. *Biochim Biophys Acta.* 2015; 1852:2706–11. <https://doi.org/10.1016/j.bbadis.2015.09.022> PMID:[26435083](https://pubmed.ncbi.nlm.nih.gov/26435083/)
7. Chen H, Xu C, Jin Q, Liu Z. S100 protein family in human cancer. *Am J Cancer Res.* 2014; 4:89–115. PMID:[24660101](https://pubmed.ncbi.nlm.nih.gov/24660101/)
8. Madsen P, Rasmussen HH, Leffers H, Honoré B, Dejgaard K, Olsen E, Kiil J, Walbum E, Andersen AH, Basse B. Molecular cloning, occurrence, and expression of a novel partially secreted protein "psoriasin" that is highly up-regulated in psoriatic skin. *J Invest Dermatol.* 1991; 97:701–12. <https://doi.org/10.1111/1523-1747.ep12484041> PMID:[1940442](https://pubmed.ncbi.nlm.nih.gov/1940442/)
9. Zhou G, Xie TX, Zhao M, Jasser SA, Younes MN, Sano D, Lin J, Kupferman ME, Santillan AA, Patel V, Gutkind JS, Ei-Naggar AK, Emberley ED, et al. Reciprocal negative regulation between S100A7/psoriasin and beta-catenin signaling plays an important role in tumor progression of squamous cell carcinoma of oral cavity. *Oncogene.* 2008; 27:3527–38. <https://doi.org/10.1038/sj.onc.1211015> PMID:[18223693](https://pubmed.ncbi.nlm.nih.gov/18223693/)
10. Nasser MW, Qamri Z, Deol YS, Ravi J, Powell CA, Trikha P, Schwendener RA, Bai XF, Shilo K, Zou X, Leone G, Wolf R, Yuspa SH, Ganju RK. S100A7 enhances mammary tumorigenesis through upregulation of inflammatory pathways. *Cancer Res.* 2012; 72:604–15. <https://doi.org/10.1158/0008-5472.CAN-11-0669> PMID:[22158945](https://pubmed.ncbi.nlm.nih.gov/22158945/)
11. West NR, Watson PH. S100A7 (psoriasin) is induced by the proinflammatory cytokines oncostatin-M and interleukin-6 in human breast cancer. *Oncogene.* 2010; 29:2083–92. <https://doi.org/10.1038/onc.2009.488> PMID:[20101226](https://pubmed.ncbi.nlm.nih.gov/20101226/)
12. Gallaher JA, Brown JS, Anderson ARA. The impact of proliferation-migration tradeoffs on phenotypic evolution in cancer. *Sci Rep.* 2019; 9:2425. <https://doi.org/10.1038/s41598-019-39636-x> PMID:[30787363](https://pubmed.ncbi.nlm.nih.gov/30787363/)
13. Lei J. Evolutionary dynamics of cancer: From epigenetic regulation to cell population dynamics—mathematical model framework, applications, and open problems. *Sci China Math.* 2020; 63:411–24. <https://doi.org/10.1007/s11425-019-1629-7>
14. Kreso A, O'Brien CA, van Galen P, Gan OI, Notta F, Brown

- AM, Ng K, Ma J, Wienholds E, Dunant C, Pollett A, Gallinger S, McPherson J, et al. Variable clonal repopulation dynamics influence chemotherapy response in colorectal cancer. *Science*. 2013; 339:543–8. <https://doi.org/10.1126/science.1227670> PMID:23239622
15. Tuasha N, Petros B. Heterogeneity of Tumors in Breast Cancer: Implications and Prospects for Prognosis and Therapeutics. *Scientifica (Cairo)*. 2020; 2020:4736091. <https://doi.org/10.1155/2020/4736091> PMID:33133722
16. Ohata Y, Shimada S, Akiyama Y, Mogushi K, Nakao K, Matsumura S, Aihara A, Mitsunori Y, Ban D, Ochiai T, Kudo A, Arii S, Tanabe M, Tanaka S. Acquired Resistance with Epigenetic Alterations Under Long-Term Antiangiogenic Therapy for Hepatocellular Carcinoma. *Mol Cancer Ther*. 2017; 16:1155–65. <https://doi.org/10.1158/1535-7163.MCT-16-0728> PMID:28246302
17. Wang Y, Mao Y, Wang C, Jiang X, Tang Q, Wang L, Zhu J, Zhao M. RNA methylation-related genes of m6A, m5C, and m1A predict prognosis and immunotherapy response in cervical cancer. *Ann Med*. 2023; 55:2190618. <https://doi.org/10.1080/07853890.2023.2190618> PMID:37042849
18. Mayakonda A, Lin DC, Assenov Y, Plass C, Koeffler HP. Maftools: efficient and comprehensive analysis of somatic variants in cancer. *Genome Res*. 2018; 28:1747–56. <https://doi.org/10.1101/gr.239244.118> PMID:30341162
19. Bonneville R, Krook MA, Kautto EA, Miya J, Wing MR, Chen HZ, Reeser JW, Yu L, Roychowdhury S. Landscape of Microsatellite Instability Across 39 Cancer Types. *JCO Precis Oncol*. 2017; 2017. <https://doi.org/10.1200/PO.17.00073> PMID:29850653
20. Thorsson V, Gibbs DL, Brown SD, Wolf D, Bortone DS, Ou Yang TH, Porta-Pardo E, Gao GF, Plaisier CL, Eddy JA, Ziv E, Culhane AC, Paull EO, et al, and Cancer Genome Atlas Research Network. The Immune Landscape of Cancer. *Immunity*. 2018; 48:812–30.e14. <https://doi.org/10.1016/j.immuni.2018.03.023> PMID:29628290
21. Malta TM, Sokolov A, Gentles AJ, Burzykowski T, Poisson L, Weinstein JN, Kamińska B, Huelsken J, Omberg L, Gevaert O, Colaprico A, Czerwińska P, Mazurek S, et al, and Cancer Genome Atlas Research Network. Machine Learning Identifies Stemness Features Associated with Oncogenic Dedifferentiation. *Cell*. 2018; 173:338–54.e15. <https://doi.org/10.1016/j.cell.2018.03.034> PMID:29625051
22. Beroukhi R, Mermel CH, Porter D, Wei G, Raychaudhuri S, Donovan J, Barretina J, Boehm JS, Dobson J, Urashima M, Mc Henry KT, Pinchback RM, Ligon AH, et al. The landscape of somatic copy-number alteration across human cancers. *Nature*. 2010; 463:899–905. <https://doi.org/10.1038/nature08822> PMID:20164920
23. Mermel CH, Schumacher SE, Hill B, Meyerson ML, Beroukhi R, Getz G. GISTIC2.0 facilitates sensitive and confident localization of the targets of focal somatic copy-number alteration in human cancers. *Genome Biol*. 2011; 12:R41. <https://doi.org/10.1186/gb-2011-12-4-r41> PMID:21527027
24. Lu Z, Li Y, Che Y, Huang J, Sun S, Mao S, Lei Y, Li N, Sun N, He J. The TGFβ-induced lncRNA TBILA promotes non-small cell lung cancer progression in vitro and in vivo via cis-regulating HGAL and activating S100A7/JAB1 signaling. *Cancer Lett*. 2018; 432:156–68. <https://doi.org/10.1016/j.canlet.2018.06.013> PMID:29908210
25. Lin M, Xia B, Qin L, Chen H, Lou G. S100A7 Regulates Ovarian Cancer Cell Metastasis and Chemoresistance Through MAPK Signaling and Is Targeted by miR-330-5p. *DNA Cell Biol*. 2018; 37:491–500. <https://doi.org/10.1089/dna.2017.3953> PMID:29485916
26. Quail DF, Joyce JA. Microenvironmental regulation of tumor progression and metastasis. *Nat Med*. 2013; 19:1423–37. <https://doi.org/10.1038/nm.3394> PMID:24202395
27. Nallasamy P, Nimmakayala RK, Parte S, Are AC, Batra SK, Ponnusamy MP. Tumor microenvironment enriches the stemness features: the architectural event of therapy resistance and metastasis. *Mol Cancer*. 2022; 21:225. <https://doi.org/10.1186/s12943-022-01682-x> PMID:36550571
28. Keir ME, Butte MJ, Freeman GJ, Sharpe AH. PD-1 and its ligands in tolerance and immunity. *Annu Rev Immunol*. 2008; 26:677–704. <https://doi.org/10.1146/annurev.immunol.26.021607.090331> PMID:18173375
29. Pardoll DM. The blockade of immune checkpoints in cancer immunotherapy. *Nat Rev Cancer*. 2012; 12:252–64. <https://doi.org/10.1038/nrc3239> PMID:22437870

30. Guo Z, Zhang R, Yang AG, Zheng G. Diversity of immune checkpoints in cancer immunotherapy. *Front Immunol.* 2023; 14:1121285. <https://doi.org/10.3389/fimmu.2023.1121285> PMID:[36960057](https://pubmed.ncbi.nlm.nih.gov/36960057/)
31. Valdés-González JA, Sánchez M, Moratilla-Rivera I, Iglesias I, Gómez-Serranillos MP. Immunomodulatory, Anti-Inflammatory, and Anti-Cancer Properties of Ginseng: A Pharmacological Update. *Molecules.* 2023; 28:3863. <https://doi.org/10.3390/molecules28093863> PMID:[37175273](https://pubmed.ncbi.nlm.nih.gov/37175273/)
32. Yang Y, Lundqvist A. Immunomodulatory Effects of IL-2 and IL-15; Implications for Cancer Immunotherapy. *Cancers (Basel).* 2020; 12:3586. <https://doi.org/10.3390/cancers12123586> PMID:[33266177](https://pubmed.ncbi.nlm.nih.gov/33266177/)
33. Mishra S, Charan M, Shukla RK, Agarwal P, Misri S, Verma AK, Ahirwar DK, Siddiqui J, Kaul K, Sahu N, Vyas K, Garg AA, Khan A, et al. cPLA2 blockade attenuates S100A7-mediated breast tumorigenicity by inhibiting the immunosuppressive tumor microenvironment. *J Exp Clin Cancer Res.* 2022; 41:54. <https://doi.org/10.1186/s13046-021-02221-0> PMID:[35135586](https://pubmed.ncbi.nlm.nih.gov/35135586/)
34. Padilla L, Dakhel S, Adan J, Masa M, Martinez JM, Roque L, Coll T, Hervas R, Calvis C, Llinas L, Buenestado S, Castellsague J, Messeguer R, et al. S100A7: from mechanism to cancer therapy. *Oncogene.* 2017; 36:6749–61. <https://doi.org/10.1038/onc.2017.283> PMID:[28825725](https://pubmed.ncbi.nlm.nih.gov/28825725/)
35. Nasser MW, Wani NA, Ahirwar DK, Powell CA, Ravi J, Elbaz M, Zhao H, Padilla L, Zhang X, Shilo K, Ostrowski M, Shapiro C, Carson WE 3rd, Ganju RK. RAGE mediates S100A7-induced breast cancer growth and metastasis by modulating the tumor microenvironment. *Cancer Res.* 2015; 75:974–85. <https://doi.org/10.1158/0008-5472.CAN-14-2161> PMID:[25572331](https://pubmed.ncbi.nlm.nih.gov/25572331/)
36. Liu C, Zheng S, Lu Z, Wang Z, Wang S, Feng X, Wang Y, Sun N, He J. S100A7 attenuates immunotherapy by enhancing immunosuppressive tumor microenvironment in lung squamous cell carcinoma. *Signal Transduct Target Ther.* 2022; 7:368. <https://doi.org/10.1038/s41392-022-01196-4> PMID:[36266269](https://pubmed.ncbi.nlm.nih.gov/36266269/)
37. Wang X, Dong Y, Zhang H, Zhao Y, Miao T, Mohseni G, Du L, Wang C. DNA methylation drives a new path in gastric cancer early detection: Current impact and prospects. *Genes Dis.* 2023; 11:847–60. <https://doi.org/10.1016/j.gendis.2023.02.038> PMID:[37692483](https://pubmed.ncbi.nlm.nih.gov/37692483/)
38. Liu J, Huang B, Ding F, Li Y. Environment factors, DNA methylation, and cancer. *Environ Geochem Health.* 2023; 45:7543–68. <https://doi.org/10.1007/s10653-023-01749-8> PMID:[37715840](https://pubmed.ncbi.nlm.nih.gov/37715840/)
39. Huang Y, Zhang W, Li Q, Wang Z, Yang X. Identification of m6A/m5C/m1A-associated LncRNAs for prognostic assessment and immunotherapy in pancreatic cancer. *Sci Rep.* 2023; 13:3661. <https://doi.org/10.1038/s41598-023-30865-9> PMID:[36871072](https://pubmed.ncbi.nlm.nih.gov/36871072/)
40. Zhang Y, Zhang X, Huang X, Tang X, Zhang M, Li Z, Hu X, Zhang M, Wang X, Yan Y. Tumor stemness score to estimate epithelial-to-mesenchymal transition (EMT) and cancer stem cells (CSCs) characterization and to predict the prognosis and immunotherapy response in bladder urothelial carcinoma. *Stem Cell Res Ther.* 2023; 14:15. <https://doi.org/10.1186/s13287-023-03239-1> PMID:[36721217](https://pubmed.ncbi.nlm.nih.gov/36721217/)
41. Zhuang H, Yu B, Tao D, Xu X, Xu Y, Wang J, Jiao Y, Wang L. The role of m6A methylation in therapy resistance in cancer. *Mol Cancer.* 2023; 22:91. <https://doi.org/10.1186/s12943-023-01782-2> PMID:[37264402](https://pubmed.ncbi.nlm.nih.gov/37264402/)